Electrocatalysis

DOI: 10.1002/ange.201306750

Pulsed-EPR Evidence of a Manganese(II) Hydroxycarbonyl Intermediate in the Electrocatalytic Reduction of Carbon Dioxide by a Manganese Bipyridyl Derivative**

Marc Bourrez, Maylis Orio, Florian Molton, Hervé Vezin, Carole Duboc, Alain Deronzier, and Sylvie Chardon-Noblat**

Abstract: *A key intermediate in the electroconversion of carbon dioxide to carbon monoxide, catalyzed by a manganese tris(carbonyl) complex, is characterized. Different catalytic pathways and their potential reaction mechanisms are investigated using a large range of experimental and computational techniques. Sophisticated spectroscopic methods including UV/Vis absorption and pulsed-EPR techniques (2P-ESEEM and HYSCORE) were combined together with DFT calculations to successfully identify a key intermediate in the catalytic cycle of* CO_2 *reduction. The results directly show the formation of a metal–carboxylic acid–*CO_2 *adduct after oxidative addition of* CO_2 *and* H^+ *to a* Mn^0 *carbonyl dimer, an unexpected intermediate.*

The chemical conversion of carbon dioxide has attracted a lot of interest because simultaneously the environmental impact of CO_2 is reduced and value is created by using CO_2 as a sustainable feedstock of carbon (CO_2 recycling).[1] Electrochemical conversion of CO_2 into valuable chemicals ranging from carbon monoxide (CO) or formic acid (HCOOH), the most straightforward products from CO_2 reduction, to synthetic fuels and high-molecular polymers, could be one of the ways to store intermittent energy as chemicals that can be transported and used on demand.[2] But efficient CO_2 reduction still remains challenging. Indeed, CO_2 is a stable and inert molecule,[3] thus high-yield CO_2 conversion reactions require efficient catalysts and energy input. If the latter is a renewable source of energy the electrochemical reduction of CO_2 can be regarded as a sustainable artificial photosynthetic process. Furthermore, CO_2 reduction is a proton-dependent process; therefore catalysts must be kinetically selective to prevent the direct hydrogen evolution reaction (proton reduction). In the past thirty years several efficient and selective metal complex catalysts for the homogeneous electrochemical reduction of CO_2 to CO have been studied. This includes systems based on Re^I,[4] Ru^{II},[5] and Os^{II}[6] polypyridyl carbonyl complexes. Just a few molecular catalysts based on Fe[7] and Mn[8] (metals abundant in the earth's crust) have been reported. As recently pointed out,[2c,9] despite the large number of investigations, most reaction mechanisms of CO_2 reduction are not yet well-known and further developments are needed.

Recently, to develop new molecular electrocatalysts with the goal of implementing a sustainable CO_2 reduction process, we explored Mn carbonyl bipyridyl complexes and we showed that $[Mn^I(L)(CO)_3Br]$ (L = bpy (2,2′-bipyridine) and dmbpy (4,4′-dimethyl-2,2′-bipyridine)) are precursors to catalysts for the electroreduction of CO_2 to CO in hydro-organic electrolyte.[8a] Shortly thereafter Kubiak and co-workers[8b] extended our results with a new substituted bpy-*t*Bu Mn carbonyl complex. The two successive overall one-electron reduction reactions of $[Mn(L)(CO)_3Br]$ are summarized in Equations (1)–(2).

$$2\,[Mn^I(L)(CO)_3Br] + 2\,e^- \rightarrow [Mn^0(L)(CO)_3]_2 + 2\,Br^- \quad (1)$$

$$[Mn^0(L)(CO)_3]_2 + 2\,e^- \rightarrow 2\,[Mn(L)(CO)_3]^- \quad (2)$$

In CO_2 and in the presence of H_2O, a particular electrocatalytic property has been characterized for $[Mn(dmby)(CO)_3Br]$. Indeed when the cyclic voltammogram (CV) of this dmbpy Mn complex was recorded under CO_2 in the presence of a weak Brönsted acid (5% water; Figure S1) the increased current responses appear on both reduction reactions [Eqs. (1) and (2)] corresponding to two distinct catalytic pathways: 1) a well-known route involving the two-electron reduced $[Mn(dmbpy)(CO)_3]^-$ species.[8] This reactivity is equivalent to the one which has been proposed for the rhenium carbonyl electrocatalyst counterparts;[4a,d,10] 2) a pathway involving the $[Mn^0(dmbpy)(CO)_3]_2$ dimer [one-electron reduced species; Equation (1)] which is unstable and reactive in the presence of CO_2 and H_2O. This type of dimeric species has never been proposed as a catalytically

---

[*] Dr. M. Bourrez, F. Molton, Dr. C. Duboc, Dr. A. Deronzier, Dr. S. Chardon-Noblat
Université Joseph Fourier-Grenoble1/CNRS
Département de Chimie Moléculaire UMR5250
Laboratoire de Chimie Inorganique Redox
Institut de Chimie Moléculaire de Grenoble FR-CNRS-2607
BP53, 38041 Grenoble cedex 09 (France)
E-mail: sylvie.chardon@ujf-grenoble.fr

Dr. M. Orio, Dr. H. Vezin
Université Lille 1, Sciences et Technologies
Laboratoire de Spectrochimie Infrarouge et Raman
UMR CNRS 8516 Bâtiment C5
59655 Villeneuve d'Ascq Cedex (France)
E-mail: maylis.orio@univ-lille1.fr

[**] The authors thank the TGE Réseau National de RPE interdisciplinaire, FR-CNRS 3443, the "Agence Nationale pour la Recherche" (grant number ANR-08-CP2D-05-01; CO2GREEN) and the Labex ARCANE (grant number ANR-11-LABX-0003-01) for financial supports. We also thank M. Stanbury for proofreading of the manuscript.

Supporting information for this article is available on the WWW under http://dx.doi.org/10.1002/anie.201306750.

active intermediate for CO_2 reduction with equivalent Re carbonyl complexes. Contrariwise, it has been recently demonstrated that, regarding electrocatalysis, the rhenium dimer $[Re(bpy)(CO)_3]_2$ is a deactivation product.[10a] Nonetheless, concerning specifically photocatalysis, it has been shown that irradiation of the $[Re(dmbpy)(CO)_3]_2$ dimer induces the homolysis of the Re–Re bond leading to $[Re(dmbpy)(CO)_3]^0$; the latter then reacts "strikingly slowly" with CO_2.[10f] This particular pathway is most likely not relevant in our case since all the solutions were continuously protected from light. Moreover, we studied the mechanism of the dimerization process of $[Mn^I(L)(CO)_3Br]$ by cyclic voltammetry and DFT calculations. We showed that the dimerization is fast and thermodynamically favored (this will be reported in detail in an upcoming paper); thus the concentration of $[Mn(dmbpy)(CO)_3]^0$ in solution is extremely low. To understand the surprising one-electron mechanism pathway for the electroreduction of CO_2 to CO, catalyzed by Mn^I dmpy tris(carbonyl) complexes, we performed in situ UV/Vis and EPR spectroscopy experiments and DFT calculations. Here we report the results of this CO_2 electrocatalytic reduction mechanistic study.

UV/Vis changes (Figures S2–S5) recorded during an exhaustive electrolysis of $[Mn^I(dmbpy)(CO)_3Br]$ at $E_{app} = -1.70$ V versus Ag/Ag^+ 10^{-2} M in CO_2 (catalytic experimental conditions; see Figure S1 in the Supporting Information) provide information about the concentration of the $[Mn^0(dmbpy)(CO)_3]_2$ dimer throughout the catalytic process. In the course of the first two hours, the concentration of the dimer regularly increases to reach a steady state which corresponds to 60 % of the concentration obtained after a quantitative exhaustive electrolysis in argon.[8a] This concentration profile characterizes the balance between the consumption of the dimer and its perpetual electroregeneration, a characteristic behavior for an electrocatalytic process.

The reaction between CO_2 and $[Mn(dmbpy)(CO)_3]_2$ dimer, the one-electron reduction product of the Mn^I initial complex [Eq. (1)] has been monitored through the specific absorbance of the dimer at 815 nm in CH_3CN electrolyte containing water, a weak proton donor (Figure S6). The decrease in absorbance (from dark green to a light orange color (Figure S7) in Ar or CO_2, is directly related to the disappearance of the dimer in solution and therefore to its reactivity. The relative absorbance changes in Ar or CO_2 demonstrate that the dimer reacts much faster with CO_2 than with water. Such reactivity has been recently proved for the two-electron reduced $[Re(t\text{Bu-bpy})(CO)_3]^-$ counterpart complex and was used to explain the high selectivity of the reduction of CO_2 to CO, preventing the proton reduction.[12] The kinetics of the dimer reaction with CO_2 depend on the presence of water. Indeed while a few minutes are required in the presence of 5 % water, about 40 minutes are necessary to transform quantitatively the dimer in CH_3CN electrolyte without added water. Finally, when an exhaustive electrolysis of the orange product solution (Figure S7; $CH_3CN + 0.1$ M TBAP) is performed at $E_{app} = -1.70$ V in the presence of 5 % H_2O and CO_2, CO is quantitatively produced for at least 1.5 h. This shows unambiguously that the product resulting from the reaction of the dimer with CO_2 is also an electrocatalytically active intermediate. Its identification was further investigated by EPR spectroscopy and theoretical calculations (DFT). Even though pulsed EPR techniques are not as widespread or commonly used as IR spectroscopy to characterize this kind of intermediate, we used it preferentially since it can provide direct and meaningful evidence about the structure of the compound. Moreover, since this electrocatalytic process requires a large amount of water which absorbs a lot in CO stretching region, implementing in situ IR spectroscopy characterization is far from straightforward.

At 100 K the CO_2 adduct compound displays a continuous-wave (cw) X-band EPR spectrum with a broad isotropic signal, a line width of about 1000 G centered at $g_{iso} = 2.001$, characteristic of an $S = 1/2$ species (Figure 1, inset). By comparison with previously published EPR studies on Mn carbonyl complexes[12] this signal has been assigned to a mononuclear low-spin d^5 Mn^{II} complex consistent with the high-field ligand character of the CO ligands.[13] Pulsed-EPR experiments (two-pulse electron spin echo envelope modulation: 2P-ESEEM and two-dimension hyperfine sublevel correlation: 2D-HYSCORE) have been conducted to get insight into the structural surroundings of the unpaired electron of this paramagnetic intermediate. For nuclei that are coupled to the electronic spin by anisotropic hyperfine interaction, 2P-ESEEM measurements have proven to be powerful tools whereas HYSCORE enables the proper assignment of quadrupolar and hyperfine couplings of the electronic spin with a large number of nuclei.[14] Measurements have been performed on frozen CH_3CN samples of the $[Mn^0(dmbpy)(CO)_3]_2$ dimer in which $^{13}CO_2$ was bubbled before or after addition of 5 % water. The 2D-HYSCORE and 2P-ESEEM spectra recorded on both samples are shown respectively in Figure 1 and Figure S8. The ESEEM spectrum before adding water reveals three main peaks (3.50, 6.90, and 14.10 MHz) attributed to the basic frequency and combination lines of ^{13}C ($I = 1/2$, $n = 3.56$ MHz) and ^1H ($I = 1/2$, $n = 14.17$ MHz) nuclei. These data evidence undoubtedly an

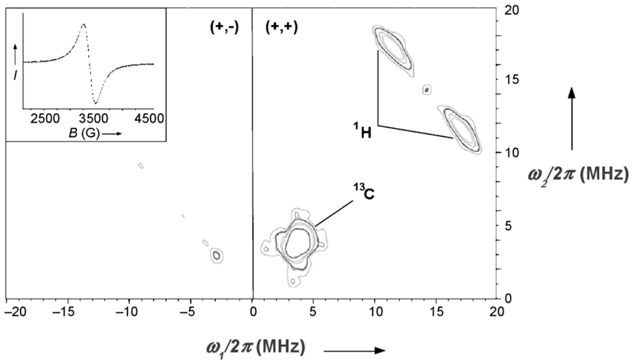

Figure 1. 2D-HYSCORE spectra of the frozen solution of $[Mn(dmbpy)(CO)_3]_2$ 0.45 mM MeCN + 0.1 M TBAP + $^{13}CO_2$ + 5 % H_2O (2.4 M) recorded at $g = 2.068$ of the cw X-band spectrum (inset) for $T = 6$ K. The time delay was set to 136 ns, a pulse length of 16 ns was used for $\pi/2$ pulses with 128 × 128 points along t_1 and t_2 directions.

interaction between the ^{13}C from $^{13}CO_2$ with the metal center, in agreement with a direct coordination of the ^{13}C nuclei to the manganese ion. It also shows that distant protons are present in the surroundings of the unpaired electron of the system. After adding water to the sample, the spectrum shows a notable increase in the peaks observed without added water, especially at 14.17 MHz, and in the appearance of a new peak at 28.50 MHz, which has been assigned to the combination line of ^{1}H nuclei.

These changes, caused by the addition of water, prove the interaction of the Mn^{II} ion of the product with protons from the weak acid (H_2O). Further information on the latter couplings was gained from HYSCORE measurements. The spectrum recorded in the presence of water is characterized by a pair of cross-peaks centered at the ^{1}H Larmor nuclear frequency. These symmetric cross-peaks appear in the $(+,+)$ quadrant, indicating weak hyperfine isotropic couplings, case with $A_{\mathrm{iso}} < 2\nu$ (^{1}H), that are estimated at 6.4 MHz. Another peak is detected in the $(+,+)$ quadrant and centered at the ^{13}C Larmor nuclear frequency. This peak characterizes a dipolar interaction between the unpaired electron of the complex and the distant ^{13}C nuclei with a coupling estimated at 1.2 MHz. This set of experimental data thus directly shows the coordination of the carbon dioxide through a metal–carbon bond and the protonation of the subsequent group in the presence of a weak acid like water. This analysis greatly supports a structure for the intermediate as being a [Mn(dmbpy)(CO)$_3$(C(O)OH)]$^+$ low-spin Mn^{II} complex bearing a hydroxycarbonyl ligand. Two isomers of this metallocarboxylic acid species could exist in solution. Indeed it has been shown that fast isomerization from *fac* to *mer* Mn^{II} tris(carbonyl) compounds occurs after oxidation of the initial corresponding *fac* halide Mn^{I} complexes.[15] Both [Mn^{II}(dmbpy)(CO)$_3$(C(O)OH)]$^+$ isomers were thus constructed and their DFT-geometry optimizations have been conducted. The two resulting structures are depicted in Figure S9 together with selected metrical parameters. As expected, the calculated free-energies for both forms predict the *mer* isomer to be lower in energy by 3.80 kcal mol^{-1}. Therefore, only calculations performed on the *mer* isomer will be further discussed (data on the *fac* isomer are provided in the Supporting Information). Electronic structure calculations were performed and the localized singly occupied molecular orbital (SOMO) is depicted in Figure 2. Not surprisingly, the SOMO is a metal-based orbital (3d$_{xy}$) and displays 90% manganese character with small contributions from the coordinating atoms because of the covalence of the metal–ligand bonds. The EPR parameters were calculated and are reported in Table S1. The computed isotropic g_{iso} value of 2.002 matches well the experimental data. The same analysis can be applied for both ^{1}H and ^{13}C hyperfine couplings: the computed values of −6.06 and −1.47 MHz compare well with the values obtained from pulse EPR measurements (6.40 and 1.20 MHz, respectively). The good agreement found between theory and experiment confirms that the *mer*-[Mn(dmbpy)(CO)$_3$(C(O)OH)]$^+$ proposed structure is relevant to describe the observed low-spin Mn^{II} intermediate.

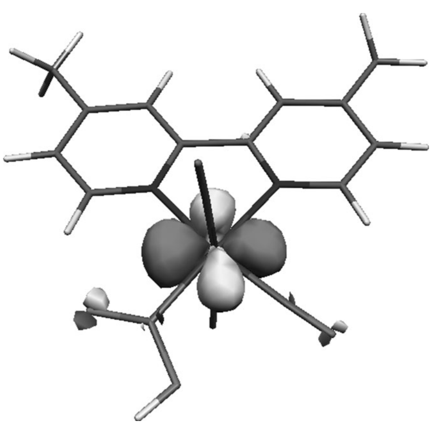

Figure 2. Localized SOMO orbital for *mer*-[Mn(dmbpy)(CO)$_3$(C(O)OH)]$^+$ isomer.

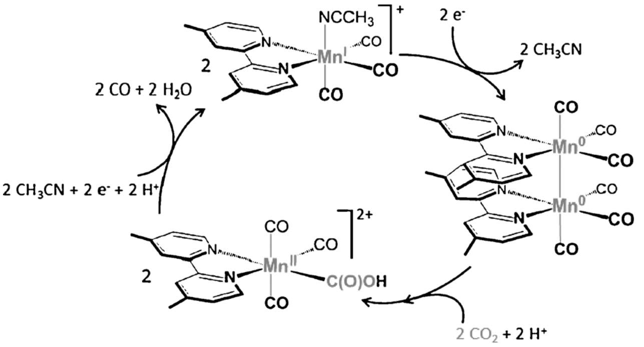

Scheme 1. Proposed electrocatalytic mechanism.

Given these results we propose the catalytic cycle in Scheme 1. At the beginning of the reaction, [Mn^{I}(L)(CO)$_3$(CH$_3$CN)]$^+$ is electrochemically reduced and the dimer is produced. Then the dimer reacts with CO_2 and a proton, most likely in a collaborative pathway as the reaction with CO_2 only, or H$^+$ only, is significantly slower. This reaction in the coordination sphere of the Mn^0 atom is a two-electron oxidative addition where two electrons are transferred from the Mn center to the "CO_2/H^{+}" moiety which leads to the mononuclear Mn^{II}-hydroxycarbonyl low-spin intermediate. Such a metallo carboxylic acid, with a direct metal–carbon bond intermediate was previously proposed for various metallic complex catalysts[7a,10c,e,16] but not characterized in great detail during electrocatalysis. Subsequently the Mn^{II} complex, which is fairly stable in solution (no significant change in the UV/Vis spectra was observed after one hour; $\lambda_{\max} = 360$ and 500 nm), is reduced into the Mn^{I} initial species in the presence of protons at the potential of the electrocatalysis and production of CO occurs. We are currently conducting the corresponding DFT calculations to determine the stability, energetics and molecular properties of the various monomeric and dimeric species; the preliminary data are in good agreement with the proposed catalytic cycle. Finally, electrocatalytic experiments performed with $^{13}CO_2$ and subsequent analysis of ^{13}C-carbon using isotope ratio gas chromatography mass spectrometry (GCMS) have been used to prove that the production of CO comes directly from CO_2.

In conclusion, this study provides a direct experimental evidence for the oxidation state of the metal and the coordination mode of CO_2 in the CO_2 adduct intermediate of the electrocatalytic process. This intermediate, which is produced from the Mn^0 carbonyl dimer species is a hydroxycarbonyl dmbpy Mn^{II} complex, one of the rare examples of Mn^{II} low-spin compounds reported in the literature. We also provide experimental data indicating that the Mn^0 carbonyl dimer is a key intermediate in this electrocatalytic process. Furthermore combining DFT calculations to pulsed-EPR investigations allows us to understand this mechanism. Since there is no precedent for such an experimentally characterized key intermediate, obtained through an one-electron reduction pathway, our work should be a good step forward to a better understanding of the mechanism of the reduction of CO_2. We also hope that these results should participate in the rational design of efficient and sustainable new catalytic devices. We are now investigating several Mn^I carbonyl complexes containing different bpy derivatives, to evaluate the influence of the bpy-type ligands, especially the electronic effects afforded by their substitution, for the electrocatalytic reduction of CO_2 particularly in terms of efficiency and selectivity.

Received: August 1, 2013
Revised: October 11, 2013

Keywords: carbon dioxide · catalysis · electrocatalysis · EPR spectroscopy · manganese

[1] See, for instance: a) G. A. Olah, A. Goeppert, G. K. S. Prakash, *J. Org. Chem.* **2009**, *74*, 487–498; b) A. A. Adesina, *Appl. Catal. A* **1996**, *138*, 345–367; c) I. Omae, *Coord. Chem. Rev.* **2012**, *256*, 1384–1405; d) W. Wang, S. P. Wang, X. B. Ma, J. L. Gong, *Chem. Soc. Rev.* **2011**, *40*, 3703–3727; e) Z. Jiang, T. Xiao, V. L. Kuznztsov, P. P. Edwards, *Philos. Trans. R. Soc. London Ser. A* **2010**, *368*, 3343–3364; f) M. Aresta in *Carbon Dioxide as a Chemical Feedstock* (Eds.: M. Aresta), Wiley-VCH, Weinheim, **2010**; g) T. Sakakura, J. C. Choi, H. Yasuda, *Chem. Rev.* **2007**, *107*, 2365–2387; h) C. S. Song, *Catal. Today* **2006**, *115*, 2–32.

[2] a) D. T. Whipple, P. J. A. Kenis, *J. Phys. Chem. Lett.* **2010**, *1*, 3451–3458; b) J. L. Inglis, B. J. MacLean, M. T. Pryce, J. G. Vos, *Coord. Chem. Rev.* **2012**, *256*, 2571–2600; c) C. Costentin, M. Robert, J. M. Saveant, *Chem. Soc. Rev.* **2013**, *42*, 2423–2436.

[3] a) G. Centi, S. Perathoner, *Catal. Today* **2009**, *148*, 191–205; b) B. Kumar, M. Llorente, J. Froehlich, T. Dang, A. Sathrum, C. P. Kubiak, *Annu. Rev. Phys. Chem.* **2012**, *63*, 541–569 (Eds.: M. A. Johnson, T. J. Martinez).

[4] a) B. P. Sullivan, C. M. Bolinger, D. Conrad, W. J. Vining, T. J. Meyer, *J. Chem. Soc. Chem. Commun.* **1985**, 1414–1416; b) J. Hawecker, J. M. Lehn, R. Ziessel, *Helv. Chim. Acta* **1986**, *69*, 1990–2012; c) S. Cosnier, A. Deronzier, J. C. Moutet, *New J. Chem.* **1990**, *14*, 831–839; d) K. A. Grice, N. X. Gu, M. D. Sampson, C. P. Kubiak, *Dalton Trans.* **2013**, *42*, 8498–8503, and references therein.

[5] a) H. Ishida, K. Tanaka, T. Tanaka, *Organometallics* **1987**, *6*, 181–186; b) H. Ishida, K. Fujiki, T. Ohba, K. Ohkubo, K. Tanaka, T. Terada, T. Tanaka, *J. Chem. Soc. Dalton Trans.* **1990**, 2155–2160; c) J. R. Pugh, M. R. M. Bruce, B. P. Sullivan, T. J. Meyer, *Inorg. Chem.* **1991**, *30*, 86–91; d) K. Tanaka, D. Ooyama, *Coord. Chem. Rev.* **2002**, *226*, 211–218; e) S. Chardon-Noblat, M. N. Collomb-Dunand-Sauthier, A. Deronzier, R. Ziessel, D. Zsoldos, *Inorg. Chem.* **1994**, *33*, 4410–4412; f) S. Chardon-Noblat, A. Deronzier, R. Ziessel, D. Zsoldos, *J. Electroanal. Chem.* **1998**, *444*, 253–260.

[6] S. Chardon-Noblat, A. Deronzier, F. Hartl, J. van Slageren, T. Mahabiersing, *Eur. J. Inorg. Chem.* **2001**, 613–617.

[7] a) M. Hammouche, D. Lexa, M. Momenteau, J. M. Saveant, *J. Am. Chem. Soc.* **1991**, *113*, 8455–8466; b) C. Costentin, S. Drouet, M. Robert, J. M. Saveant, *Science* **2012**, *338*, 90–94.

[8] a) M. Bourrez, F. Molton, S. Chardon-Noblat, A. Deronzier, *Angew. Chem.* **2011**, *123*, 10077–10080; *Angew. Chem. Int. Ed.* **2011**, *50*, 9903–9906; b) J. M. Smieja, M. D. Sampson, K. A. Grice, E. E. Benson, J. D. Froehlich, C. P. Kubiak, *Inorg. Chem.* **2013**, *52*, 2484–2491.

[9] D. J. Cheng, F. R. Negreiros, E. Apra, A. Fortunelli, *ChemSusChem* **2013**, *6*, 944–965.

[10] a) E. E. Benson, C. P. Kubiak, *Chem. Commun.* **2012**, *48*, 7374–7376; b) T. Scheiring, A. Klein, W. Kaim, *J. Chem. Soc. Perkin Trans. 2* **1997**, 2569–2571; c) K. Y. Wong, W. H. Chung, C. P. Lau, *J. Electroanal. Chem.* **1998**, *453*, 161–169; d) D. H. Gibson, X. L. Yin, H. Y. He, M. S. Mashuta, *Organometallics* **2003**, *22*, 337–346; e) P. Christensen, A. Hamnett, A. V. G. Muir, J. A. Timney, *J. Chem. Soc. Dalton Trans.* **1992**, 1455–1463; f) Y. Hayashi, S. Kita, B. S. Brunschwig, E. Fujita, *J. Am. Chem. Soc.* **2003**, *125*, 11976–11987.

[11] J. M. Smieja, E. E. Benson, B. Kumar, K. A. Grice, C. S. Seu, A. J. M. Miller, J. M. Mayer, C. P. Kubiak, *Proc. Natl. Acad. Sci. USA* **2012**, *109*, 15646–15650.

[12] A. T. Radosevich, J. G. Melnick, S. A. Stoian, D. Bacciu, C. H. Chen, B. M. Foxman, O. V. Ozerov, D. G. Nocera, *Inorg. Chem.* **2009**, *48*, 9214–9221.

[13] D. F. Shriver, P. W. Atkins in *Inorganic Chemistry*, Oxford University Press, **2001**, pp. 227–236.

[14] a) T. Prisner, M. Rohrer, F. MacMillan, *Annu. Rev. Phys. Chem.* **2001**, *52*, 279–313; b) J. Harmer, G. Mitrikas, A. Schweiger in *High Resolution EPR Biological Magnetic Resonance, Vol. 28* (Eds.: G. Hanson, L. Berliner), Springer, New York, **2009**, pp. 13–61.

[15] J. P. Bullock, E. Carter, R. Johnson, A. T. Kennedy, S. E. Key, B. J. Kraft, D. Saxon, P. Underwood, *Inorg. Chem.* **2008**, *47*, 7880–7887.

[16] a) E. Fujita, C. Creutz, N. Sutin, D. J. Szalda, *J. Am. Chem. Soc.* **1991**, *113*, 343–353; b) E. Fujita, L. R. Furenlid, M. W. Renner, *J. Am. Chem. Soc.* **1997**, *119*, 4549–4550.